Electronic Supplementary Material (ESI) for Journal of Materials Chemistry C.

Supporting information

Asymmetric anthracene hosts decorated with naphthobenzofurocarbazole for highly efficient deep blue organic light-emitting diodes and low efficiency roll-off

Yeonju Jeong,‡[a] Kyo Min Hwang,‡[a] Jae Hee Lee,‡[c] Min Jeong Kwon,[c] Taekyung Kim*[ab] and Wan Pyo Hong*[c]

[a]Department of Information Display, Hongik University, Seoul, 04066, Korea

[b]Department of Materials Science and Engineering, Hongik University, Sejong, 30016, Korea

[c]Department of Chemistry, Gachon University 1342, Seongnam-daero, Sujeong-gu, Seongnam-si, Gyeonggi-do, Korea

Page

I. Supplementary Figures, Scheme and Tables

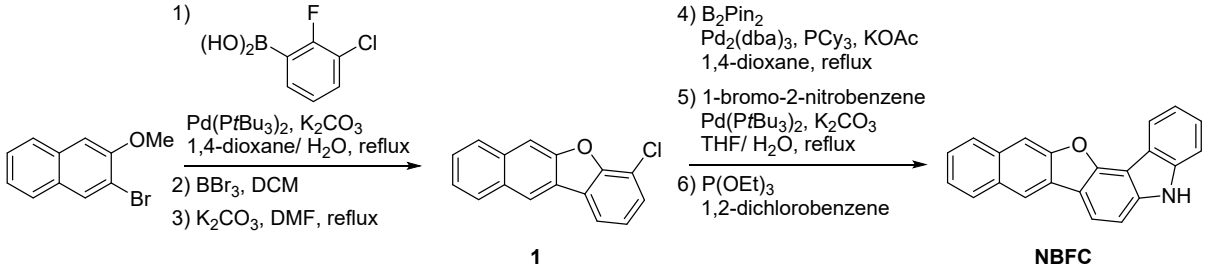

Scheme S1. Synthetic route of NBFC

Synthesis of 4-chloronaphtho[2,3-b]benzofuran **1**:

2-bromo-3-methoxynaphthalene (11.85 g, 50 mmol) and 3-chloro-2-fluorophenylboronic acid (9.59 g, 55 mmol) were dissolved in 300 ml of 1,4-dioxane: water (2:1) mixture containing potassium carbonate (K_2CO_3) (3.0 eq.) and 1.0 mol% of bis(tri-*tert*-butylphosphine)palladium(0) [($PdP tBu_3)_2$] as a catalyst. Under a nitrogen atmosphere, the reaction mixture was refluxed for 12 h. After cooling, the reaction mixture was extracted with ethyl acetate (200 ml) and washed with water. The organic layer was dried over anhydrous sodium sulfate (Na_2SO_4) and filtered through a short silica plug. The desired fractions were evaporated under reduced pressure and dried.

The corresponding product was dissolved in 400 ml of dichloromethane (DCM) and cooled to -10 ℃ under nitrogen atmosphere. Boron tribromide (BBr_3) (1.2 eq.) was slowly added and the reaction mixture was stirred at room temperature for 24 h. The mixture was slowly quenched with saturated sodium bicarbonate ($NaHCO_3$) solution and extracted with DCM. The organic layer was dried over anhydrous Na_2SO_4 and filtered through a short silica plug. The solvent was evaporated under reduced pressure and dried.

The corresponding product and K_2CO_3 (1.5 eq.) were dissolved in 100 ml of *N*,*N*-dimethylformamide. The mixture was stirred at 160 ℃ under a nitrogen condition for 8 h. After cooling to room temperature, the mixture was extracted with diethyl ether and rinsed with water. The organic layer was dried over anhydrous Na_2SO_4 and filtered through a short silica plug. The solvent was evaporated under reduced pressure and dried to afford 4-chloronaphtho[2,3-*b*]benzofuran **1** (4.6 g, 18.2 mmol) which was further crystallized from

diethyl ether-pentane (3.8 g, 15.0 mmol). ^{1}H NMR (500 MHz, $CDCl_3$) δ 8.39 (s, 1H), 8.03 (dd, *J* = 8.1, 0.6 Hz, 1H), 8.01 – 7.97 (m, 2H), 7.95 (dd, *J* = 7.6, 1.1 Hz, 1H), 7.58 – 7.48 (m, 3H), 7.31 (t, *J* = 7.8 Hz, 1H). ^{13}C NMR (125 MHz, $CDCl_3$) δ 154.55, 153.34, 133.25, 130.29, 128.38, 128.32, 127.91, 126.16, 125.73, 124.99, 124.65, 123.61, 119.71, 119.54, 117.02, 107.53.

Synthesis of 5*H*-naphtho[2',3':4,5]furo[3,2-*c*]carbazole (**NBFC**):

tris(dibenzylideneacetone)dipalladium (1.83 g, 2.0 mmol) and tricyclohexyl phosphine (1.12g, 4.0 mmol) dissolved in 80 ml of 1,4-dioxane. The mixture was stirred at room temperature under a nitrogen condition for 10 min. 4-chloronaphtho[2,3-*b*]benzofuran (5.05 g, 20 mmol), 4,4,4′,4′,5,5,5′,5′-Octamethyl-2,2′-bi-1,3,2-dioxaborolane (B_2Pin_2) (10.15 g, 40 mmol) and potassium acetate (KOAc) (3.84 g, 40 mmol) were added and the reaction was refluxed under nitrogen atmosphere. After 24 h, the reaction mixture was cooled and evaporated under reduced pressure. Then the reaction mixture was diluted with dichloromethane and filtered through a short silica plug. The solvent was evaporated under reduced pressure, and the product was dried to afford 4,4,5,5-tetramethyl-2-(naphtho[2,3-*b*]benzofuran-4-yl)-1,3,2-dioxaborolane, which was crystallized from diethyl ether-pentane.

The corresponding product (6.88 g, 20 mmol) and 1-bromo-2-nitrobenzene (4.44 g, 22 mmol) were dissolved in 80 ml of 1,4-dioxane: water (2:1) mixture containing K_2CO_3 (4.0 eq.) and 1.0 mol% of $(PdP^tBu_3)_2$ as a catalyst. Under a nitrogen atmosphere, the reaction mixture was stirred at reflux for 15 h. After cooling, the reaction mixture was extracted with ethyl acetate and rinsed with deionized water. The organic layer was dried over anhydrous Na_2SO_4, and filtered through a short silica plug. The solvent was evaporated under reduced pressure and the desired product was further purified by column chromatography yield 4-(2-nitrophenyl)naphtho[2,3-*b*]benzofuran (5.23 g, 15.4 mmol).

Triethyl phosphite [$P(OEt)_3$] (10.6 ml, 61.6 mmol) was added to a solution of 4-(2-nitrophenyl)naphtho[2,3-*b*]benzofuran (5.23 g, 15.4 mmol) in 1,2-dichlorobenzene (10 ml). The reaction mixture was stirred for 12 hours at 160 °C under a nitrogen atmosphere. The reaction mixture was concentrated to a brown paste by vacuum distillation to afford 5*H*-naphtho[2',3':4,5]furo[3,2-*c*]carbazole (NBFC), which was crystallized from DCM-pentane (2.68 g, 8.72 mmol). 1H NMR (500 MHz, THF-d_8) δ 10.80 (brs, 1H), 8.46 – 8.41 (m, 2H), 8.10 (d, 1H, J = 8.5 Hz), 8.09 (m, 1H), 8.04 – 8.00 (m, 2H), 7.52 (dt, J = 8.1, 0.8 Hz, 1H), 7.49 – 7.41 (m, 4H), 7.30 (ddd, J = 8.0, 7.2, 1.0 Hz, 1H). ^{13}C NMR (125 MHz, THF-d_8) δ 156.22,

153.79, 142.70, 140.89, 133.10, 131.80, 128.73, 128.64, 127.50, 126.30, 125.66, 124.94, 123.03, 121.71, 120.39, 119.02, 117.99, 115.48, 111.59, 109.25, 107.55, 107.34.

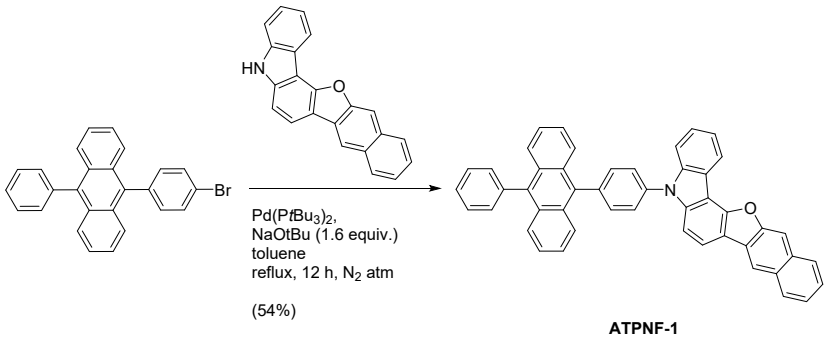

Scheme S2. Synthesis of 5-(4-(10-phenylanthracen-9-yl)phenyl)-5H-naphtho[2',3':4,5]furo[3,2-c]carbazole (**ATPNF-1**)

In a 100 mL two neck round-bottomed flask, a mixture of 9-(4-bromophenyl)-10-phenylanthracene (1.00 g, 2.44 mmol), NBFC (0.79 g, 2.56 mmol), and sodium *tert*-butoxide (NaO^{t}Bu) (0.47 g, 4.88 mmol) was added in 20 mL of *m*-xylene. The reaction mixture was stirred under a nitrogen atmosphere for 20 min and added 1.0 mol% of $(PdP^tBu_3)_2$ as a catalyst. The reaction mixture was then stirred at reflux for 8 h. After cooling, the solvent was removed under vacuum and the crude mixture was extracted in chloroform and deionized water. The organic layer was dried over anhydrous Na_2SO_4, and filtered through a short silica plug, and the solvent was evaporated under reduced pressure. The resulting product was further purified by toluene recrystallization and obtained as a white solid (0.84 g, 1.32 mmol). ^{1}H NMR (500 MHz, $CDCl_3$) δ 8.69 (d, J = 7.6 Hz, 1H), 8.46 (s, 1H), 8.18 – 8.13 (m, 2H), 8.07 (dd, J = 12.6, 7.8 Hz, 2H), 7.90 (dd, J = 10.3, 8.5 Hz, 4H), 7.80-7.76 (m, 4H), 7.75 (d, J = 8.2 Hz, 1H), 7.69 – 7.64 (m, 3H), 7.61-7.57 (m, 2H), 7.57 – 7.49 (m, 5H), 7.48 – 7.45 (m, 2H), 7.42-7.39 (m, 2H). ^{13}C NMR (125 MHz, $CDCl_3$) δ 155.51 (s), 152.94 (s), 142.22 (s), 140.78 (s), 138.94, 138.85, 137.71, 136.94 (s), 135.85, 133.01 (s), 132.09 (s), 131.30 (s), 130.58 (s), 129.96 (s), 128.48 (s), 128.07 (s), 127.90 (s), 127.60 (s), 127.23, 127.21, 126.67 (s), 126.33 (s), 126.05 (s), 125.44 (s), 125.17 (s), 124.32 (s), 122.95 (s), 121.23 (s), 121.02 (s), 118.57 (s), 117.60 (s), 116.07, 110.07 (s), 108.92 (s), 107.16 (s), 105.56 (s). MS (ESI) m/z: found 635.2269. Calculated for $C_{48}H_{29}NO$: 635.2249.

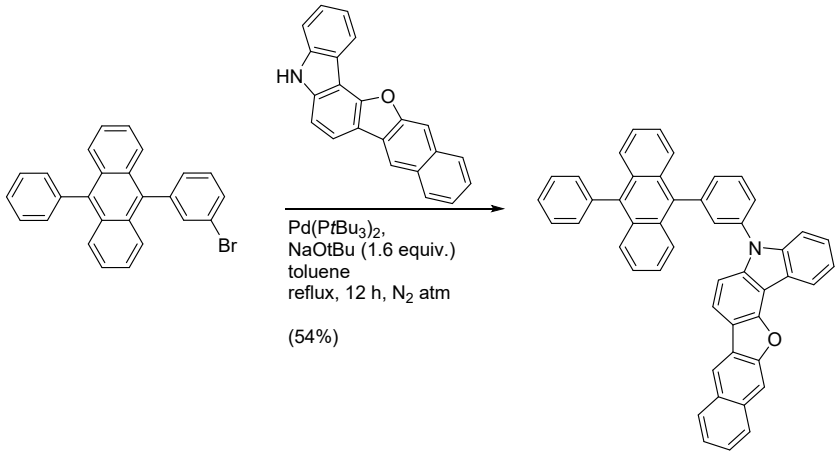

ATPNF-2

Scheme S3. Synthesis 5-(3-(10-phenylanthracen-9-yl)phenyl)-5*H*-naphtho[2',3':4,5]furo[3,2-c]carbazole (**ATPNF-2**)

In a 100 mL two neck round bottomed flask, a mixture of 9-(3-bromophenyl)-10-phenylanthracene (1.00 g, 2.44 mmol), NBFC (0.79 g, 2.56 mmol), and NaO^{t}Bu (0.47 g, 4.88 mmol) was added in 20 mL of *m*-xylene. The reaction mixture was stirred under a nitrogen atmosphere for 20 min and added 1.0 mol% of (PdP^{t}Bu$_3$)$_2$ as a catalyst. The reaction mixture was then stirred at reflux for 8 h. After cooling, the solvent was removed under vacuum and the crude mixture was extracted in chloroform and deionized water. The organic layer was dried over anhydrous Na_2SO_4, and filtered through a short silica plug, and the solvent was evaporated under reduced pressure. The resulting product was further purified by toluene recrystallization and obtained as white solid (0.84 g, 1.32 mmol). ^{1}H NMR (500 MHz, $CDCl_3$) δ 8.64 – 8.58 (m, 1H), 8.39 (s, 1H), 8.11 – 7.99 (m, 4H), 7.95 – 7.85 (m, 4H), 7.82 (t, *J* = 1.7 Hz, 1H), 7.76 (d, *J* = 8.8 Hz, 2H), 7.70 – 7.67 (m, 2H), 7.67 – 7.56 (m, 4H), 7.55 – 7.45 (m, 8H), 7.40 (ddd, *J* = 8.7, 6.5, 1.2 Hz, 2H). ^{13}C NMR (125 MHz, $CDCl_3$) δ 155.43, 152.83, 142.01, 141.26, 140.57, 138.86, 137.84, 137.77, 135.50, 132.04, 131.28, 131.23, 130.75, 130.51, 130.06, 129.94, 129.91, 129.83, 128.47, 128.43, 128.02, 127.85, 127.57, 127.21, 126.49, 126.25, 126.18, 126.00, 125.52, 125.13, 125.10, 124.26, 122.88, 121.19, 120.96, 118.53, 117.52, 116.00, 109.94, 108.87, 107.09, 105.42. MS (ESI) m/z: found 635.2269. Calculated for $C_{48}H_{29}NO$: 635.2271.

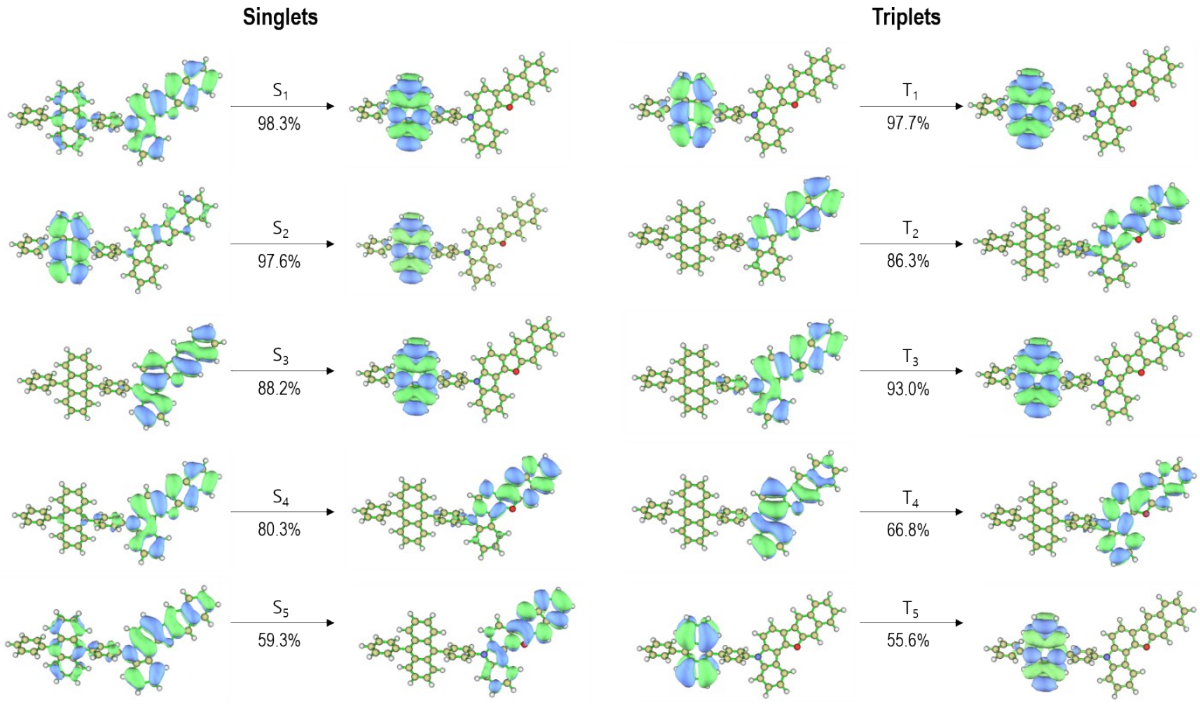

Figure S1. The natural transition orbitals of the first five singlet and triplet states of ATPNF-1

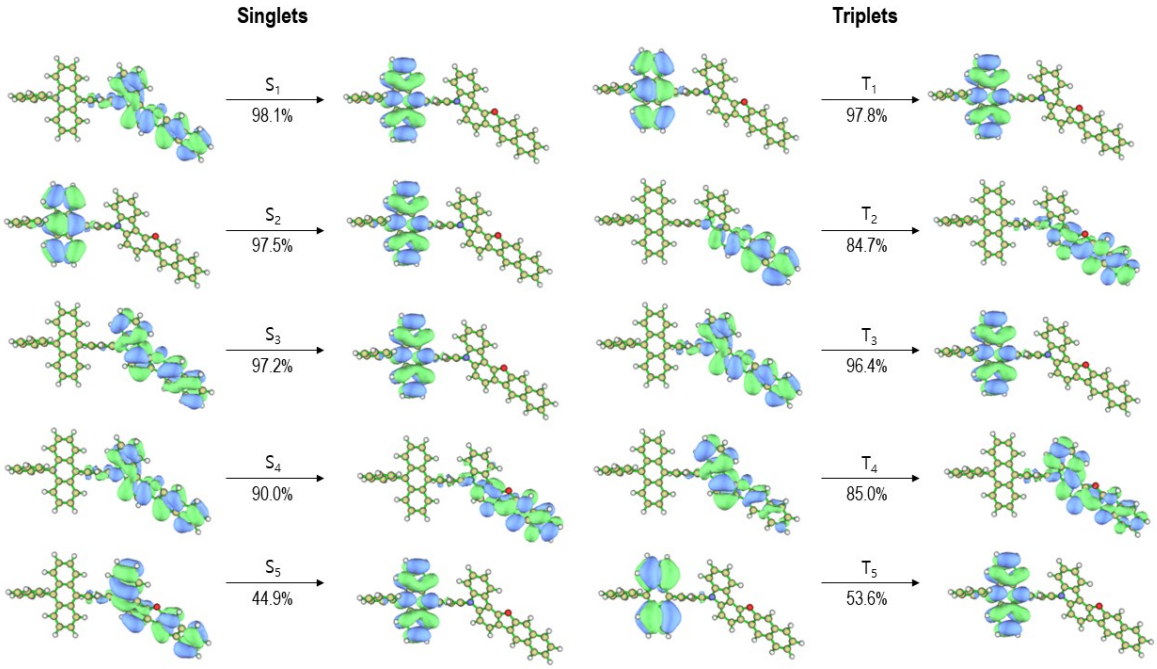

Figure S2. The natural transition orbitals of the first five singlet and triplet states of ATPNF-2

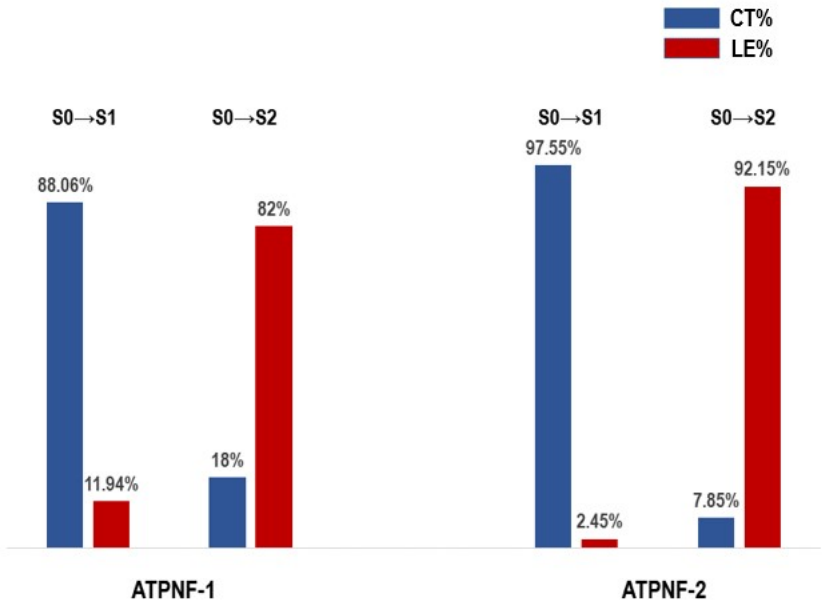

Figure S3. The proportions of LE and CT of ATPNF-1 and ATPNF-2 calculated by Multiwfn 3.8(dev)

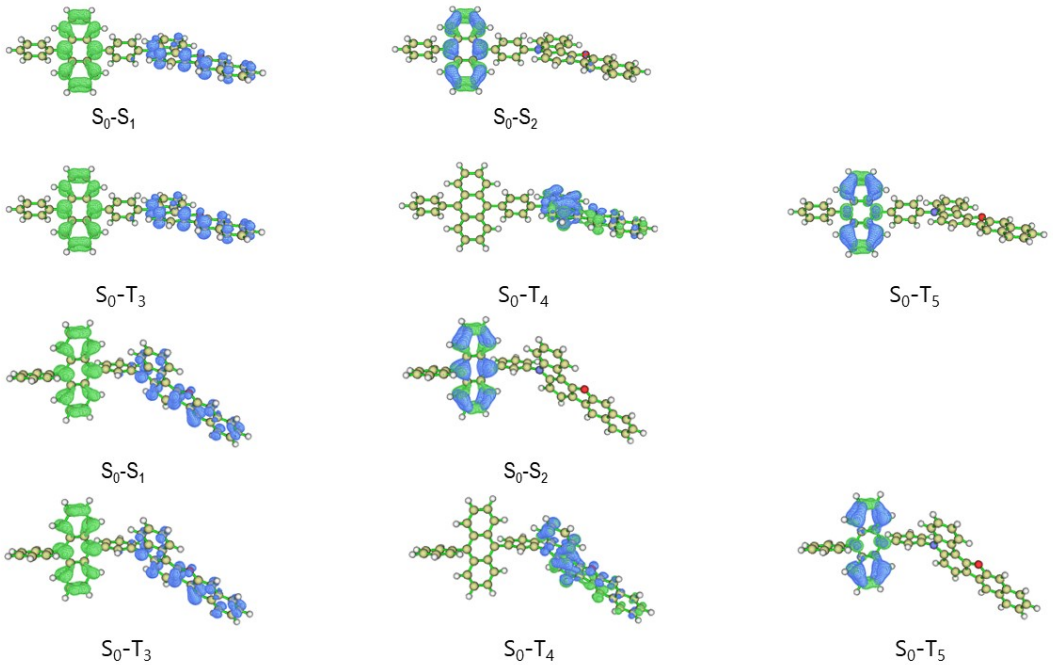

Figure S4. Isosurface of the hole (blue) and electron (green) distribution calculated by Multiwfn 3.8(dev) of S_0 to $S_{1/2}$ and S_0 to $T_{3/4/5}$ for ATPNF-1 and ATPNF-2

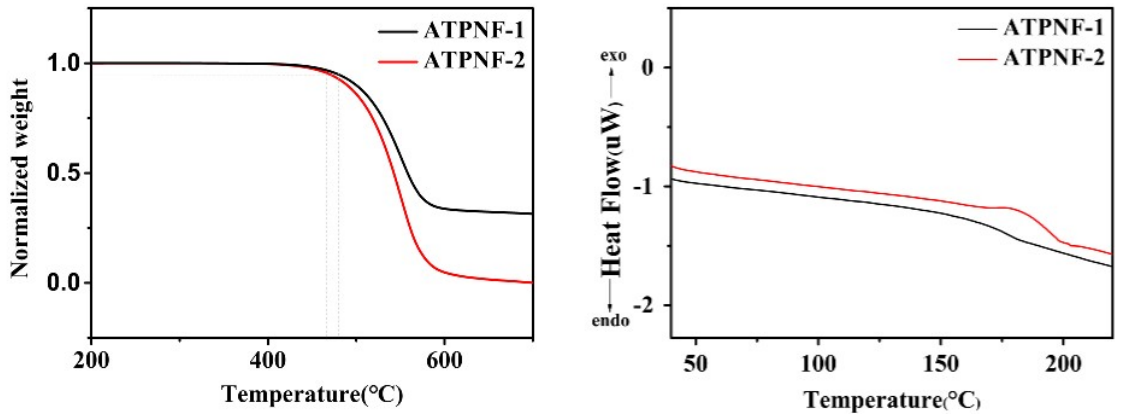

Figure S5. TGA and DSC of ATPNF-1 and ATPNF-2

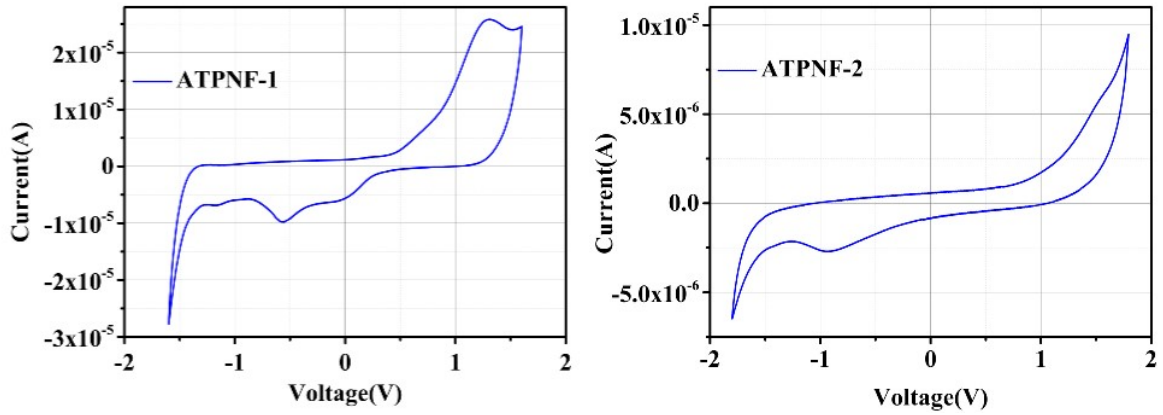

Figure S6. The cyclic voltammograms of ATPNF-1 and ATPNF-2 in CH_2Cl_2 solution containing 0.1 M TBAP electrolytes, scanning rate: 0.1 V/s

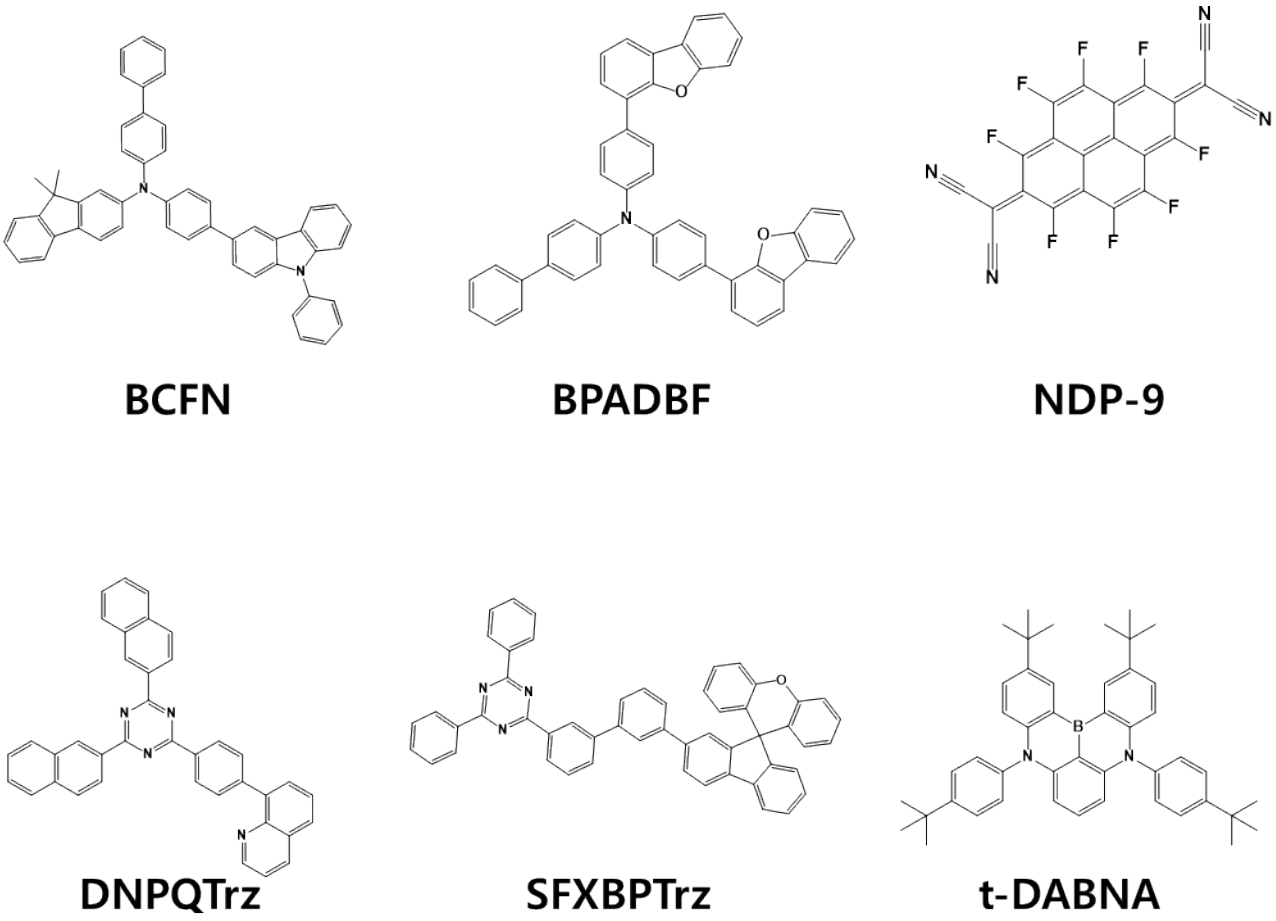

Figure S7. Molecular structures. BCFN and NDP-9 were utilized as hole-injecting layer, and BCFN was used as hole-transporting layer either. DNPQTrz was used as electron-transporting layer, BPADBF and SFXBPTrz as electron-blocking layer and hole-blocking layer. t-DABNA was used as dopant in ATPNF-1-D and ATPNF-2-D

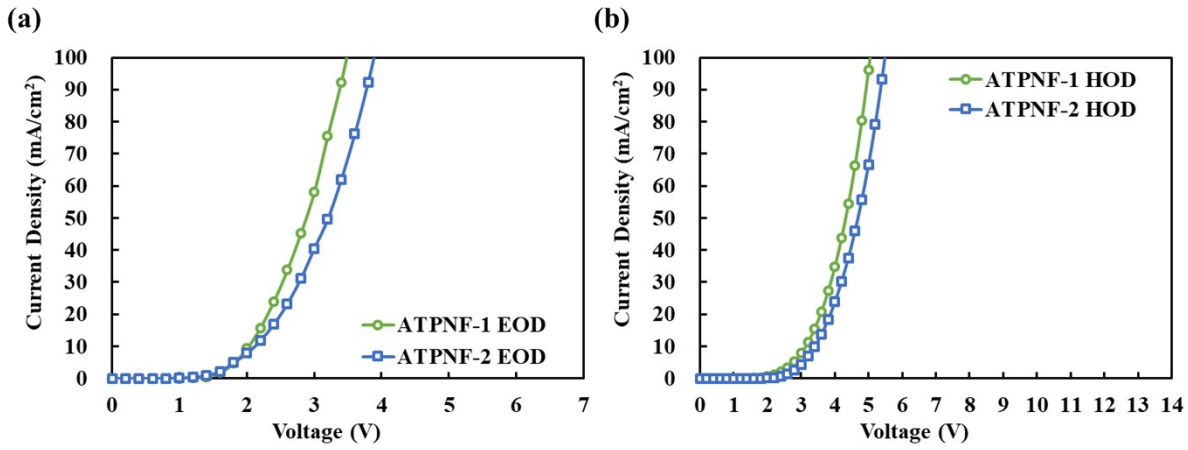

Figure S8. *J-V* characteristic of a) electron only device (EOD) b) hole only device (HOD) and

of ATPNF-1-ND and ATPNF-2-ND

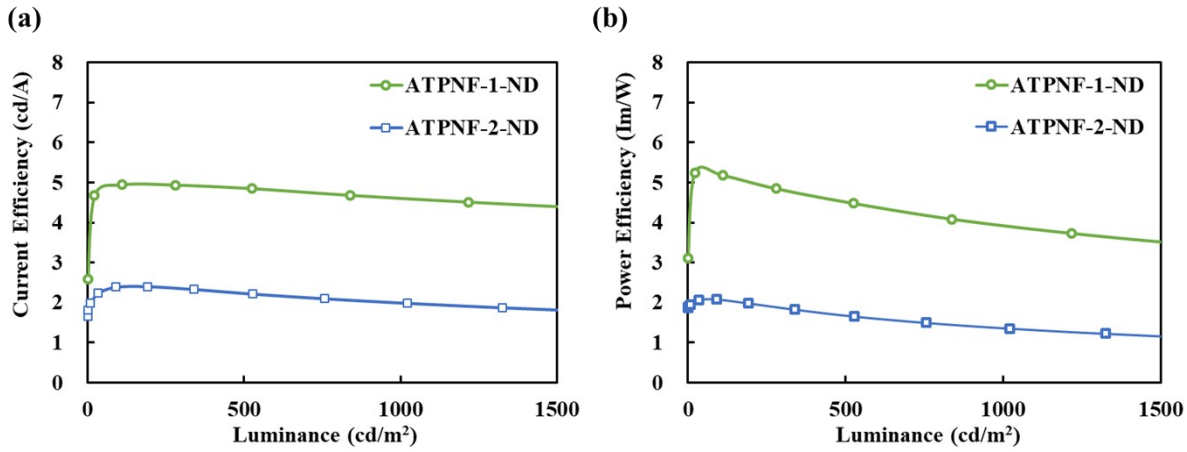

Figure S9. CE-luminance-PE curves of ATPNF-1-ND and ATPNF-2-ND

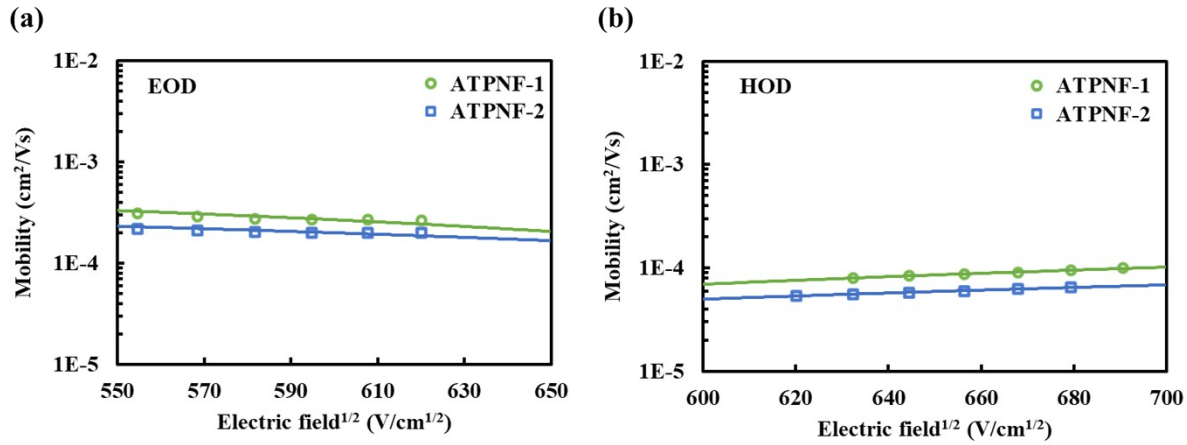

Figure S10. Mobility of ATPNF-1-ND and ATPNF-2-ND calculated from SCLC region in a) EOD and b) HOD, respectively

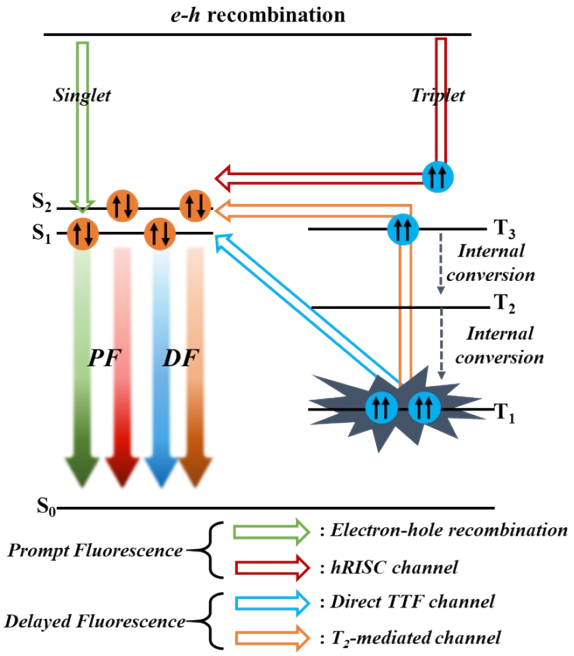

Figure S11. Photophysical dynamics of the ATPNF-1-ND and ATPNF-2-ND

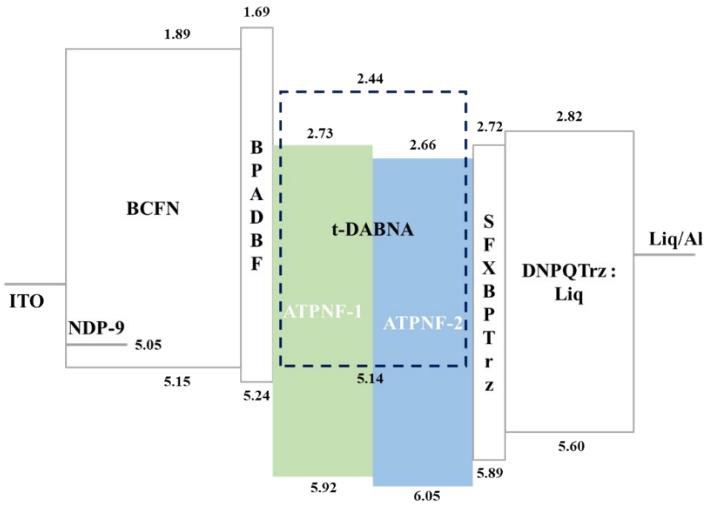

Figure S12. Device structure and energy diagram of *t*-DABNA doped ATPNF-1 and ATPNF-2 device (ATPNF-1-D and ATPNF-2-D)

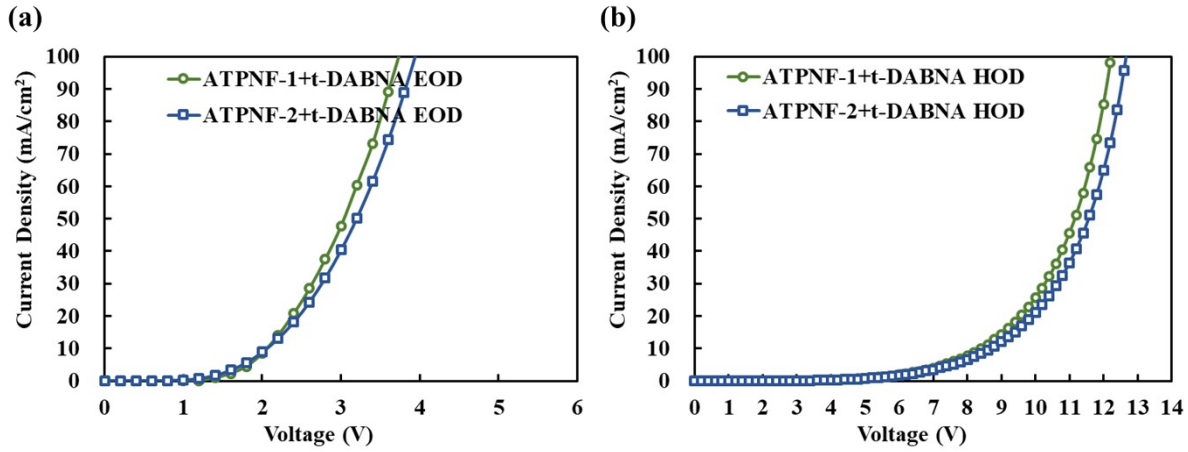

Figure S13. *J-V* characteristic of a) EOD and b) HOD of ATPNF-1-D and ATPNF-2-D

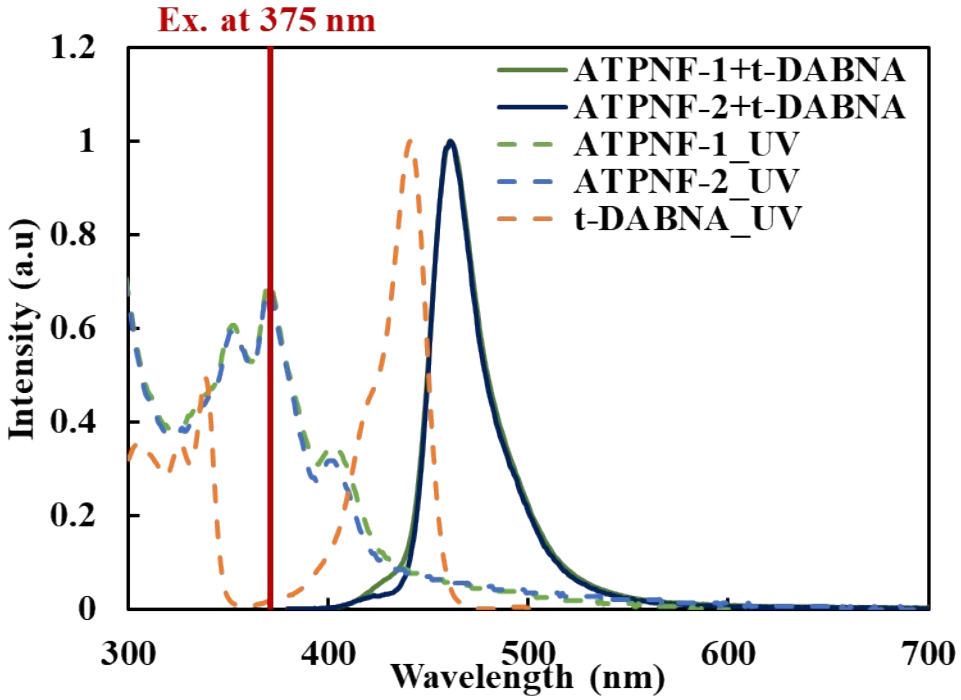

Figure S14. Photoluminescence curve of doped ATPNF-1 and ATPNF-2 film excited at 375 nm, and UV-vis of doped ATPNF-1 and ATPNF-2 film and t-DABNA solution (in toluene)

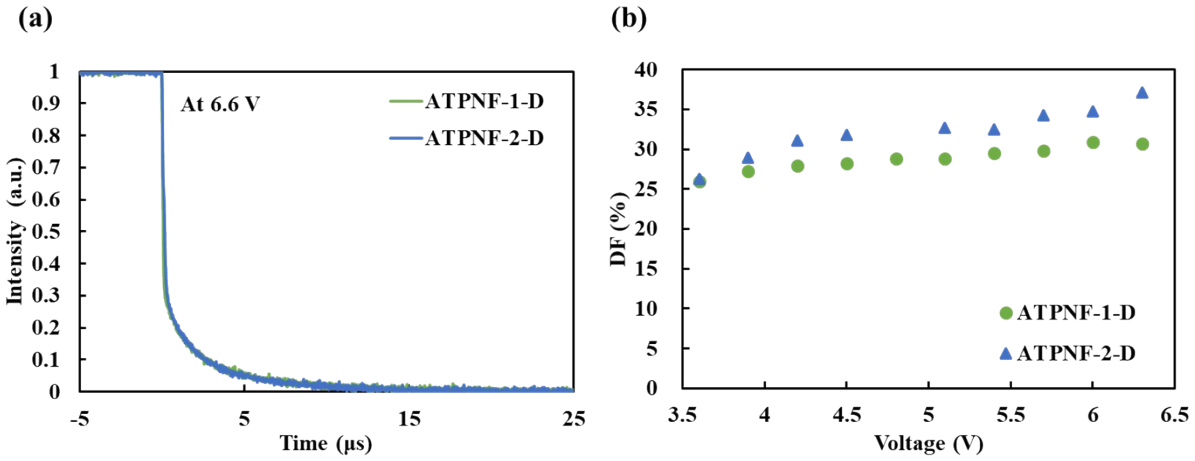

Figure S15. a) TrEL response at 6.6 V and b) DF portion of ATPNF-1-D and ATPNF-2-D

Compound	Excited State	Energy (eV)	λ (nm)	Oscillator strength	Wave function (MOs involved in the transitions)
ATPNF-1	S1	3.07	403	0.057	HOMO→LUMO
	S2	3.16	392	0.2017	HOMO-1→LUMO
	S3	3.55	348	0.0333	HOMO-2→LUMO, HOMO→LUMO+1
	S4	3.55	348	0.3747	HOMO-2→LUMO, HOMO→LUMO+1
	S5	3.74	330	0.0305	HOMO-2→LUMO+1, HOMO→LUMO+1
ATPNF-2	S1	3.04	406	0.0151	HOMO→LUMO
	S2	3.16	392	0.2109	HOMO-1→LUMO
	S3	3.51	352	0.0003	HOMO-2→LUMO
	S4	3.55	348	0.4054	HOMO→LUMO+1
	S5	3.74	331	0.0139	HOMO-3→LUMO

Table S1. Calculated electronic excitation energies, oscillator strengths and MO transition contributions for ATPNF-1 and ATPNF-2 using the B3LYP functional with the 6-31G(d,p) basis set

ATPNF-1

Solvents	ε	n	$f(\varepsilon,n)$	λ_a (nm)	λ_f (nm)	ν_a-ν_f (cm^{-1})
Toluene	2.38	1.494	0.014	373.8	432.0	3604
1,4-Dioxane	2.21	1.420	0.021	373.4	432.8	3675
Chloroform	4.81	1.443	0.149	373.1	433.2	3718
Ethyl acetate	6.02	1.372	0.200	372.9	433.0	3722

Tetrahydrofuran	7.58	1.407	0.210	372.7	432.8	3725
Dichloromethane	8.93	1.424	0.217	372.3	433.8	3807
Dimethyl formamide	37	1.427	0.276	371	436.2	4028
Acetonitrile	37.5	1.344	0.305	371	436.8	4060

ATPNF-2

Solvents	ε	n	$f(\varepsilon,n)$	λ_a (nm)	λ_f (nm)	ν_a-ν_f (cm^{-1})
Toluene	2.38	1.494	0.014	374.2	431.6	3556
1,4-Dioxane	2.21	1.420	0.021	373.7	432.2	3621
Chloroform	4.81	1.443	0.149	373.3	433.4	3665
Ethyl acetate	6.02	1.372	0.200	372.8	432.4	3695
Tetrahydrofuran	7.58	1.407	0.210	372.8	432.2	3698
Dichloromethane	8.93	1.424	0.217	372.7	434.4	3809
Dimethyl formamide	37	1.427	0.276	373.1	435.2	3824
Acetonitrile	37.5	1.344	0.305	370.8	435.6	4011

Table S2. Detailed absorption and emission peak positions of ATPNF-1 and ATPNF-2 in different solvents.

Device	γ_{e-h}	Φ_{PL} (%)	η_{out} (%)	EUE (%)	f_{DF} (%)	η_{PF} (%)	η_{DF} (%)	η_S (%)	η_{hRISC} (%)	$\eta_{TTF-hRISC}$ (%)	η_{TTF} (%)
ATPNF-1	1	54.6	20.0	63.6	28.1	45.8	17.9	25	20.8	13.4	4.5
ATPNF-2	1	42.0	20.0	47.7	31.9	32.5	15.2	25	7.5	11.4	3.8

Table S3. The subdivided proportions that contribute to radiative singlet exciton efficiency of ATPNF-1-ND and ATPNF-2-ND

Device	V_{op} [a] (V)	EQE_{max} (%)	CE_{max} (cd/A)	PE_{max} (lm/W)	λ_{max} (nm)	FWHM (nm)	CIE_{xy} [b]	Roll-off [c] (%)
ATPNF-1		8.0	6.7	7.0	463	31	0.13, 0.10	0.49
ATPNF-2		7.8	6.1	5.1	462	30	0.13, 0.09	0.25

a) Operational voltage at 1 mA/m^2, b) At luminance 1000 cd/m^2, and c) 1-(EQE at 1000 cd/m^2 / EQE_{max})

Table S4. The EL properties of ATPNF-1-D and ATPNF-2-D

Compound	Von	EQEmax/ @1000 cd/m^2 (Roll-off (%))	ELmax	CIE(x,y)	Reference
This Work	**2.9**	**7.0/6.67 (4.8)**	**446**	**(0.15, 0.07)**	
PTPC	3.1	6.78/6.18 (8.9)	411	(0.157, 0.059)	*Mater. Chem. Front.* **2022**, *6*, 2085
P2MPC	3.1	7.15/5.65 (21.0)	-	(0.157, 0.064)	*J. Mater. Chem. C.* **2022**, *10*, 9621
ATDBF	2.6	7.93/7.23 (8.8)	439	(0.15, 0.06)	*Adv. Opt. Mater.* **2022**, *10*, 2200256
3-CzPOPPI	2.9	5.08/4.44 (12.6)	436	(0.156, 0.061)	*J. Mater. Chem. C.* **2018**, *6*, 3584
CSiTPI	3.2	7.1/5.3 (25.4)	404	(0.16, 0.06)	*Adv. Opt. Mater.* **2021**, *9*, 2100965
PCZTZ	3.2	6.57/-	-	(0.17, 0.07)	*Adv. Opt. Mater.* **2017**, *5*, 1700747
CSiTPI	3.2	7.10/5.30 (25.4)	404	(0.160, 0.06)	*Adv. Opt. Mater.* **2021**, *9*, 2100965
C2MPI	3.9	6.97/-	404	(0.161, 0.06)	*J. Mater. Chem. C.* **2023**, *11*, 1733
PTPC	3.1	6.78/6.18 (8.2)	411	(0.157, 0.06)	*Mater. Chem. Front.* **2022**, *6*, 2085
2FPPIDPA	2.8	6.73/4.01 (40.4)	420	(0.156, 0.055)	*Org. Mater.* **2020**, *02*, 011
TPBCzC2	3.4	4.78/-	423	(0.159, 0.06)	*ACS Appl. Mater. Interfaces* **2020**, *12*, 46366
TFPBI	3.0	5.74/4.80 (16.4)	448	(0.152, 0.054)	*J. Mater. Chem. C.* **2019**, *7*, 592
PPi-Mid	3.1	4.60/4.08 (11.3)	436	(0.154, 0.058)	*ACS Appl. Mater. Interfaces* **2018**, *10*, 9629
4-PPI-SBF	2.75	5.29/-	424	(0.155, 0.058)	*Dyes Pigm.* **2019**, *163*, 213
SAFpCN	3.2	4.63/3.31 (28.5)	432	(0.153, 0.054)	*J. Mater. Chem. C.* **2021**, *9*, 6251
TPIN	3.0	3.71/3.70 (0.0)	443	(0.151, 0.08)	*Dyes Pigm.* **2022**, *200*, 110135
MBAn-(4)-F	3.6	6.11/1.30 (78.7)	440	(0.155, 0.058)	*Dyes Pigm.* **2018**, *148*, 329
m-BBTPI	3.2	3.63/3.36 (7.4)	428	(0.160, 0.06)	*RSC Adv.* **2015**, *5*, 18067
PhImPOtBuCz	4.4	3.42/-	419	(0.150, 0.06)	*Chem. Eng. J.* **2022**, *429*, 132327
TPINCz	3.1	5.95/-	448	(0.157, 0.084)	*Chem. Sci.* **2017**, *8*, 3599
p-PO15NCzDPA	2.8	6.40/5.58 (12.8)	444	(0.151,0.066)	*Chem. Eng. J.* **2020**, *393*, 124694
2PPIAn	3.0	8.9/-	444	(0.150, 0.060)	*ACS Appl. Mater. Interfaces* **2020**, *12*, 15422
SP	3.0	11.3/7.0 (38.1)	436	(0.158, 0.07)	*Chem. Eng. J.* **2022**, *440*, 135911

Table S5. The non-doped deep blue devices with CIEy ≤ 0.07 reported and present work

Equation S1.

$$\eta_{PF} = EUE - \eta_{DF} \tag{1}$$

$$f_{DF} = \frac{\eta_{DF}}{\eta_{PF} + \eta_{DF}} \tag{2}$$

$$\eta_{hRISC} = \eta_{PF} - \eta_s \tag{3}$$

$$\eta_{DF} = \eta_{TTF-hRISC} + \eta_{TTF} \tag{4}$$

$$\frac{\eta_{TTF-hRISC}}{\eta_{TTF}} = \frac{3k_{m-hRISC}}{k_{IC}^{Tn} + k_{m-hRISC}} \left(If.\ k_{IC}^{Tn} \ll k_{m-hRISC}\right) \tag{5}$$

II. Measurements

Photophysical, thermal and electrochemical property measurements

All reactions were performed under a nitrogen atmosphere unless otherwise noted. Reactions were monitored by thin layer chromatography (TLC) using Kieselgel 60 F254 silica gel plates. Flash chromatography was performed over silica gel 60, 230-400 mesh, with the designated solvents. The relative abundance of the isomers was determined using a 500 MHz nuclear magnetic resonance spectrometer (NMR; JNM-ECZ500R, Jeol Ltd., Tokyo, Japan) serviced by the Center for Bionano Materials Research at Gachon University (Seongnam, Korea). UV-vis absorption spectra were recorded on a UV-1900 spectrometer (Shimadzu). PL spectra were recorded on a Hitachi F-7100 fluorescence spectrophotometer. Differential scanning calorimetry (DSC) was performed on a TA DSC Q2000 at a heating rate of 10 ℃ min^{-1} under nitrogen. HPLC analysis was performed using a Waters Alliance 2695 series HPLC and a UV-vis detector. Thermogravimetric analysis (TGA) was performed on a TA SDT 650 instrument at a heating rate of 10 ℃ min^{-1} under nitrogen. The temperature at 5% weight loss was used as the decomposition temperature (T_d). Cyclic voltammetry (CV) was carried out on a WPG100e (WonATech) at room temperature with ferrocenium-ferrocene (Fc^+/Fc) as the internal standard. The oxidative scans were performed using 0.1 M n-Bu_4NPF_6 ($TBAPF_6$) in deoxygenated dichloromethane as the supporting electrolyte. The cyclic voltammograms were

obtained at a scan rate of 0.1 V s^{-1}.

Lippert-Mataga analysis

The energy difference of the fluorescence maximum relative to the absorption maximum as a function of the solvent orientation parameter $f(\varepsilon,n)$ has been used as a measure of the change in dipolemoment between the excited state and the ground state. Based on the Lippert-Mataga equation, the difference between the dipole moment of the excited and ground state ($\mu_e - \mu_g$) can be estimated from the slope of a plot of $v_a - v_f$ versus $f(\varepsilon,n)$:

$$hc(v_a - v_f) = hc(v_a^o - v_f^o) + \frac{2(\mu_e - \mu_g)}{a_o^3}^2 f(\varepsilon,n)$$ or

$$\mu_e = \mu_g + \{\frac{hca_o^3}{2} \cdot \left[\frac{d(v_a - v_f)}{df(\varepsilon,n)}\right]\}^{1/2}$$

where μ_e is the dipole moment of the excited state, μ_g is the dipole moment of the ground state, h is Planck's constatnt, c is the speed of light, a_0 is the radius of the Onsager cavity and $v_a - v_f$ is the Sokes shift. $f(\varepsilon,n)$ is the orientational polarizability of the solvent, defined as follows:

$$f(\varepsilon,n) = \frac{\varepsilon - 1}{2\varepsilon + 1} - \frac{n^2 - 1}{2n^2 - 1}$$

where ε and n are the dielectric constant and the refractive index of the solvent, respectively. The μ_e value are estimated to be 8.3D in low-polarity solvents and 16.1D in high-polarity solvents for ATPNF-1. Similarly, the μ_e values ATPNF-2 are calculated to be 9.1D and 15.4D

III. ^{1}H NMR of ATPNF-1 and ATPNF-2 in $CDCl_3$

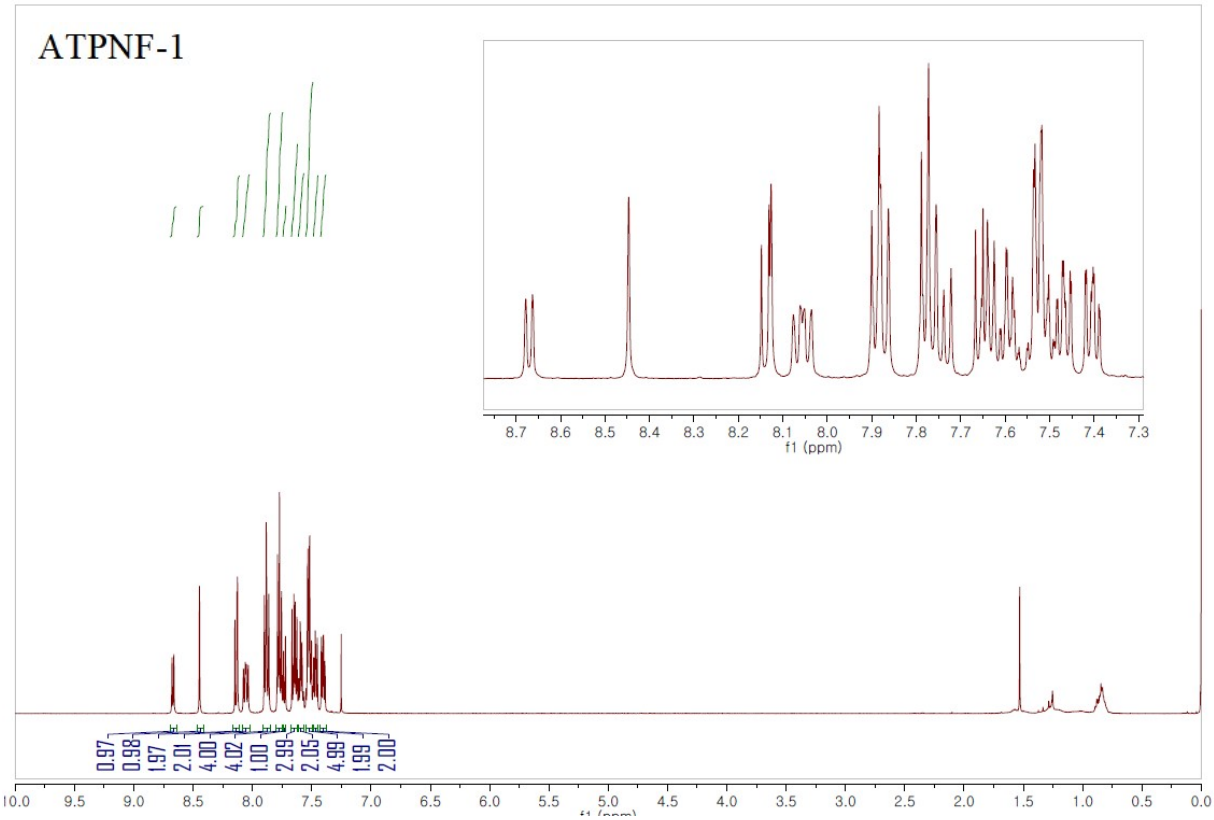

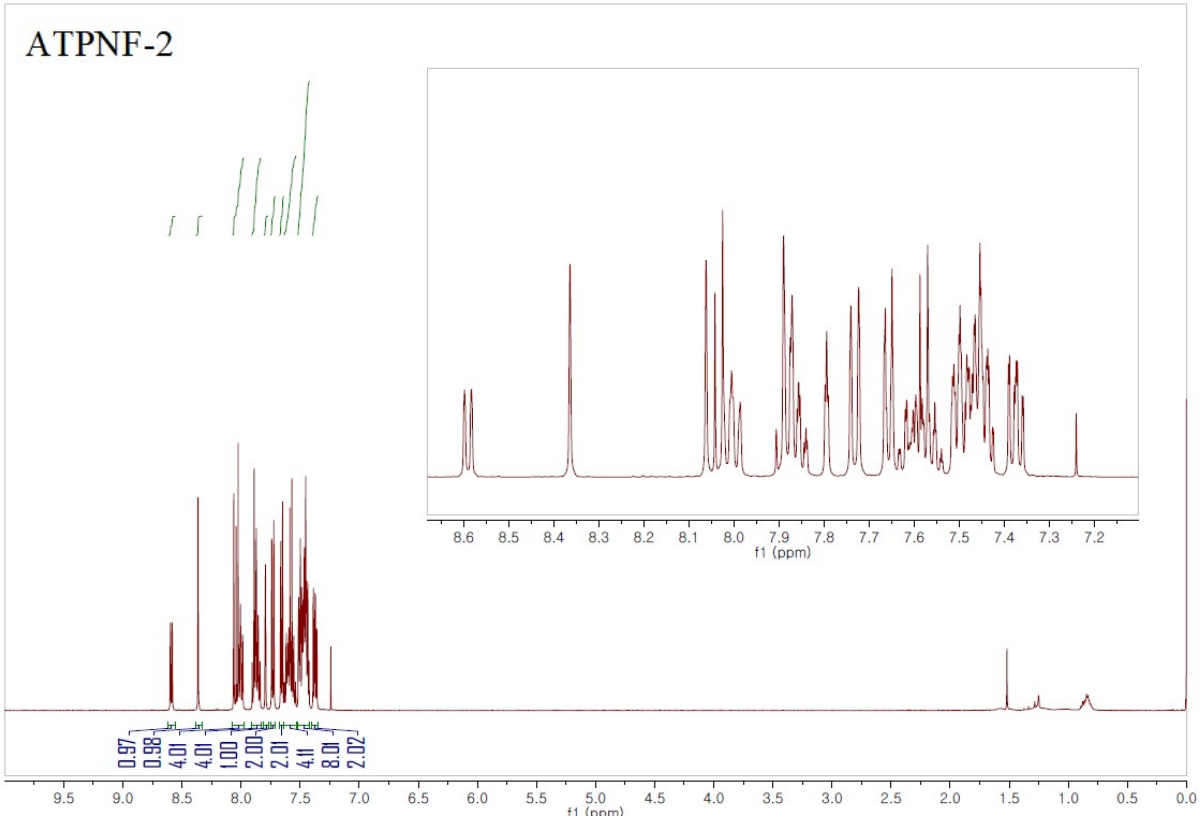

IV. ^{13}C NMR of ATPNF-1 and ATPNF-2 in $CDCl_3$

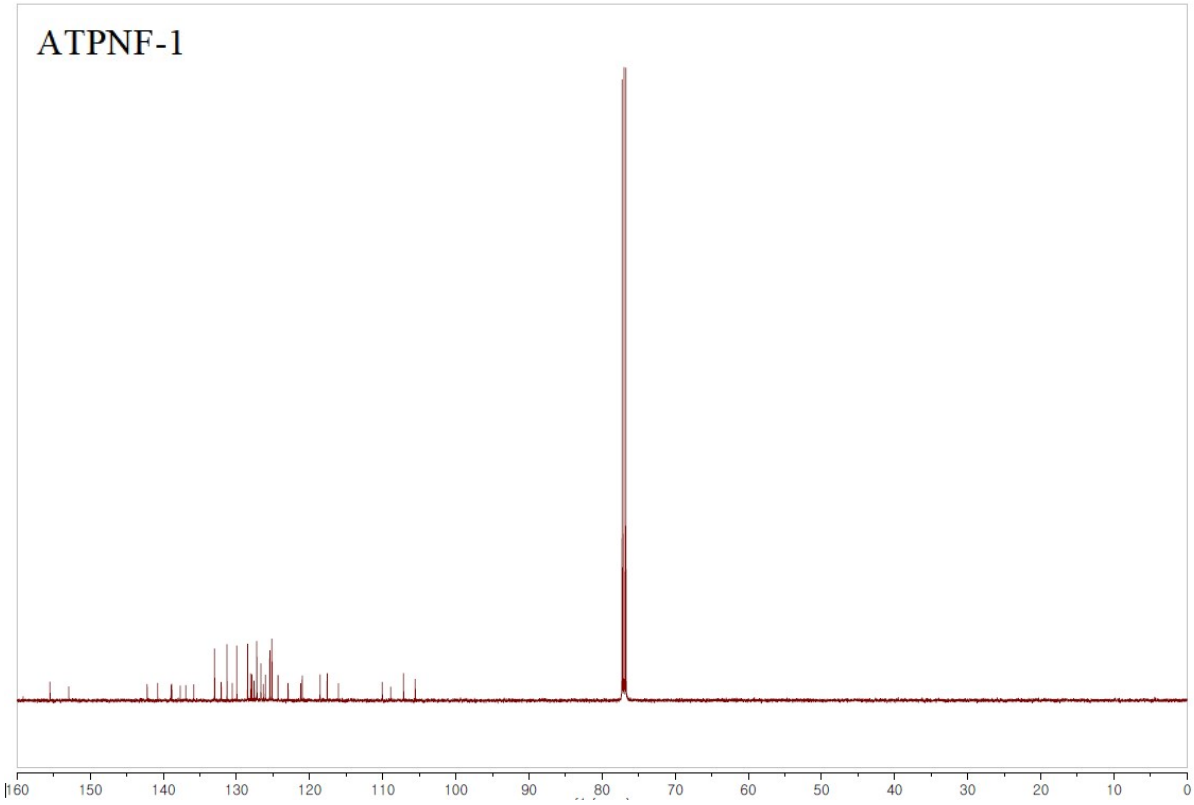

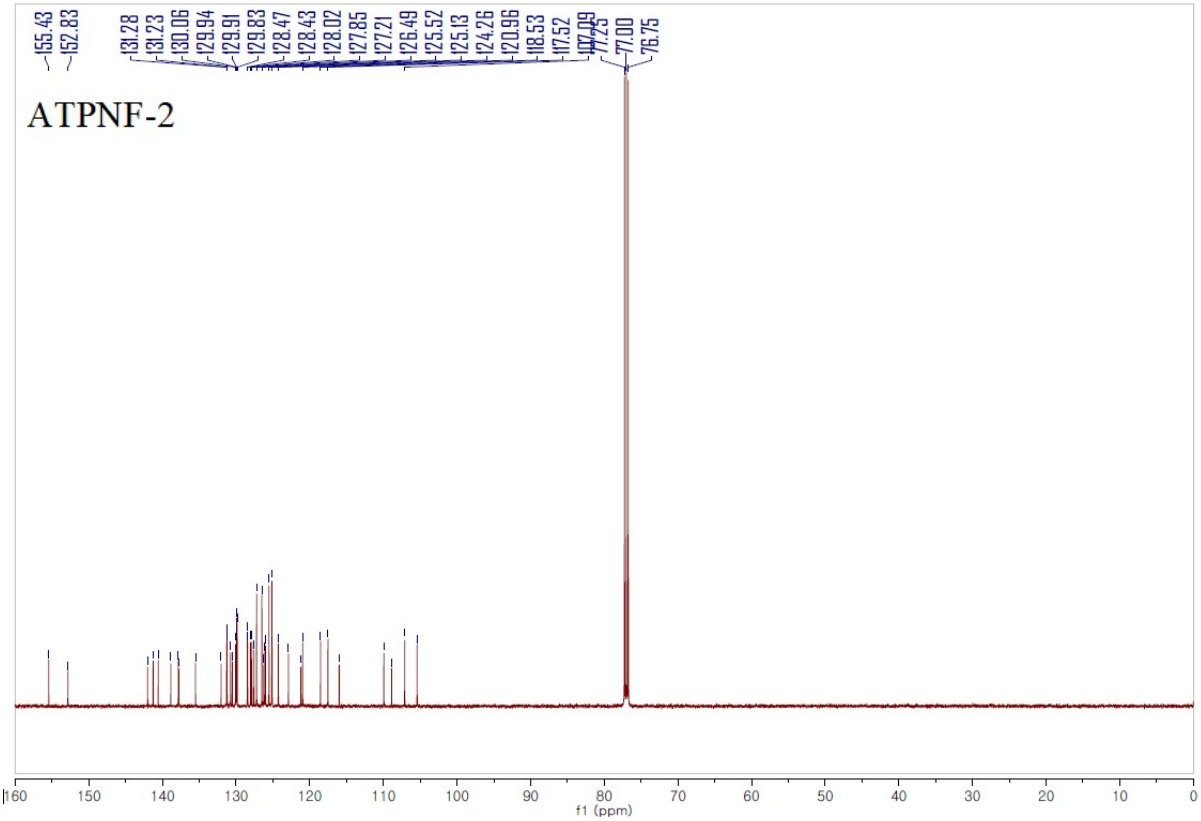

V. HR-MS of ATPNF-1 and ATPNF-2

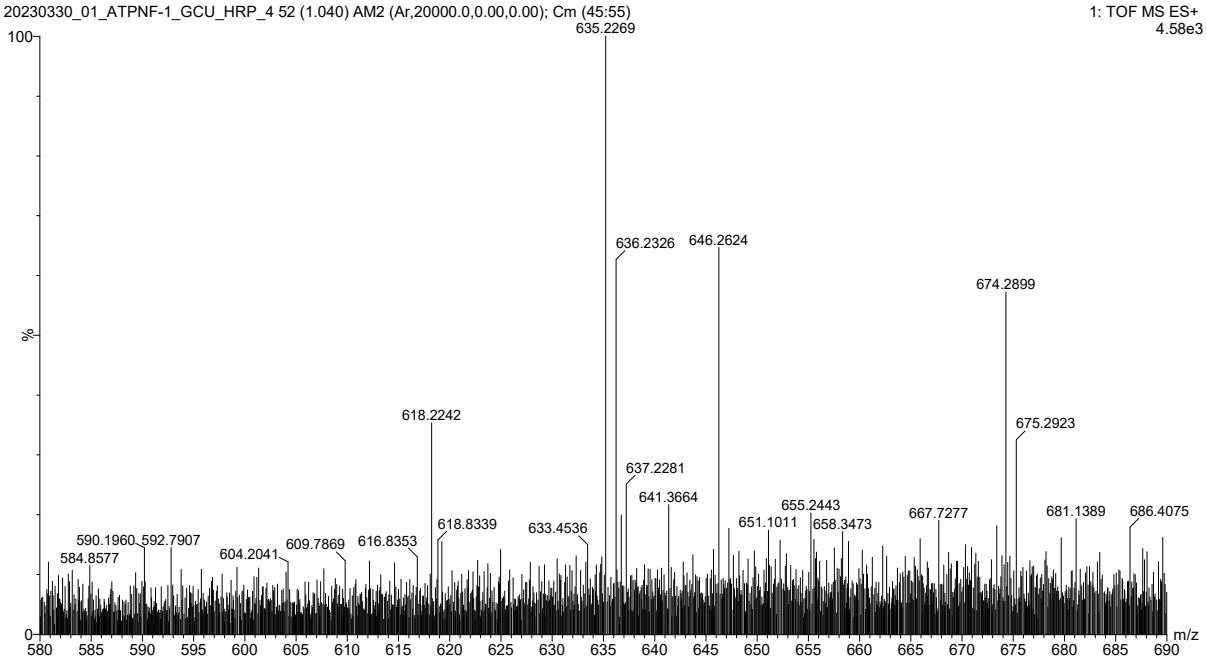

Elemental Composition Report

Single Mass Analysis

Tolerance = 5.0 PPM / DBE: min = -9.0, max = 100.0

Element prediction: Off
Number of isotope peaks used for i-FIT = 3

Monoisotopic Mass, Odd and Even Electron Ions
78 formula(e) evaluated with 1 results within limits (up to 50 closest results for each mass)
Elements Used:
C: 0-50 H: 0-130 N: 0-2 O: 0-2

Minimum:					-9.0		
Maximum:		5.0	5.0	100.0			
Mass	Calc. Mass	mDa		PPM	DBE	i-FIT	
Norm	Conf(%)	Formula					
635.2269	635.2249	2.0	3.1	35.0	332.2	n/a	n/a
	C48 H29 N O						

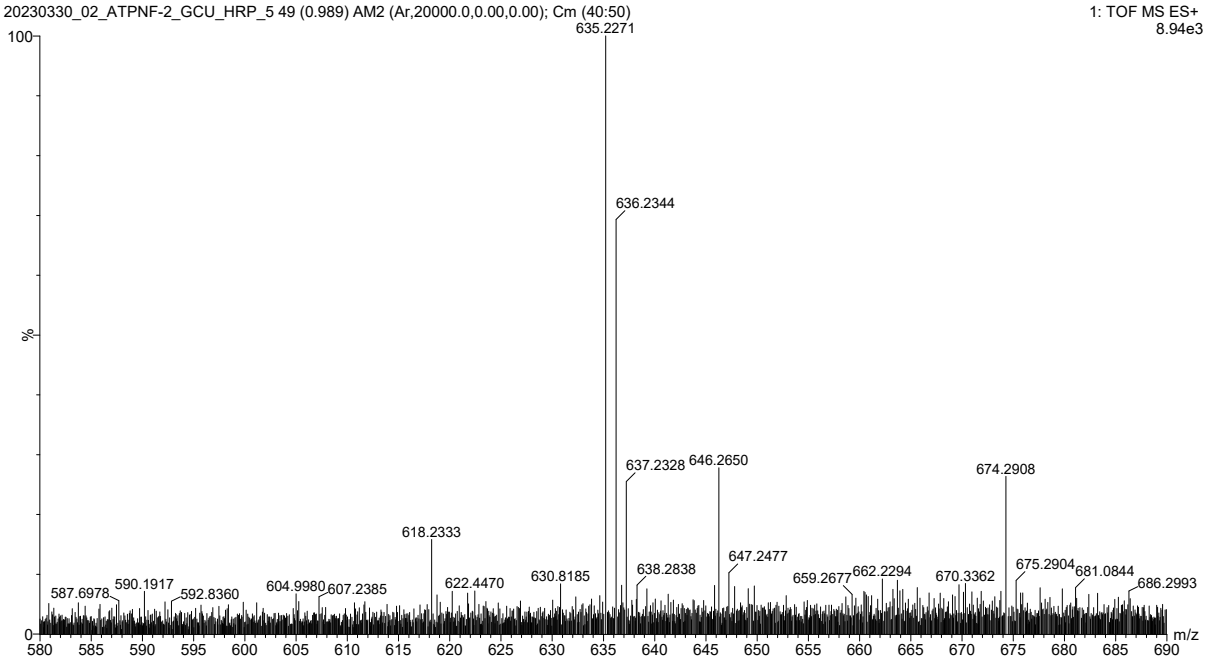

Elemental Composition Report

Single Mass Analysis
Tolerance = 5.0 PPM / DBE: min = -9.0, max = 100.0
Element prediction: Off

Number of isotope peaks used for i-FIT = 3

Monoisotopic Mass, Odd and Even Electron Ions
78 formula(e) evaluated with 1 results within limits (up to 50 closest results for each mass)
Elements Used:
C: 0-50 H: 0-130 N: 0-2 O: 0-2

Minimum:					-9.0		
Maximum:		5.0	5.0	100.0			
Mass	Calc. Mass	mDa		PPM	DBE	i-FIT	
Norm	Conf(%)	Formula					
635.2271	635.2249	2.2	3.5	35.0	298.7	n/a	n/a
C48 H29 N O							

VI. HPLC of ATPNF-1 and ATPNF-2

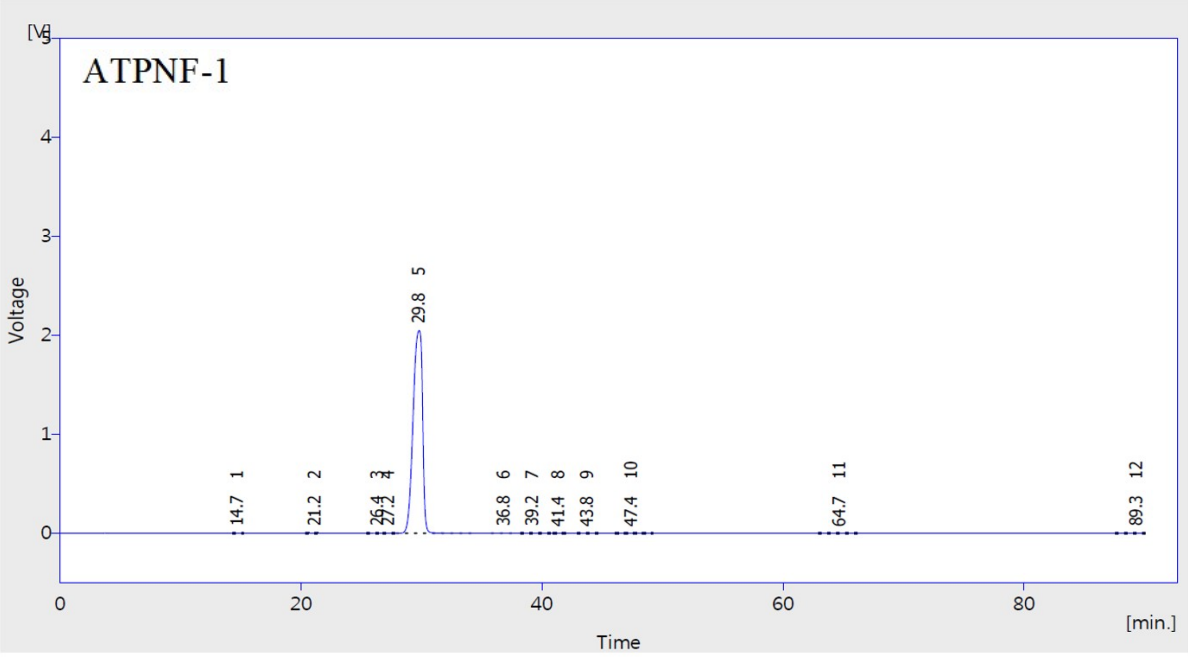

Column : Shiseido MG C18 4.6* 150mm, 5 um_Method : ACN_MeOH 7_3 0.5ml_90min

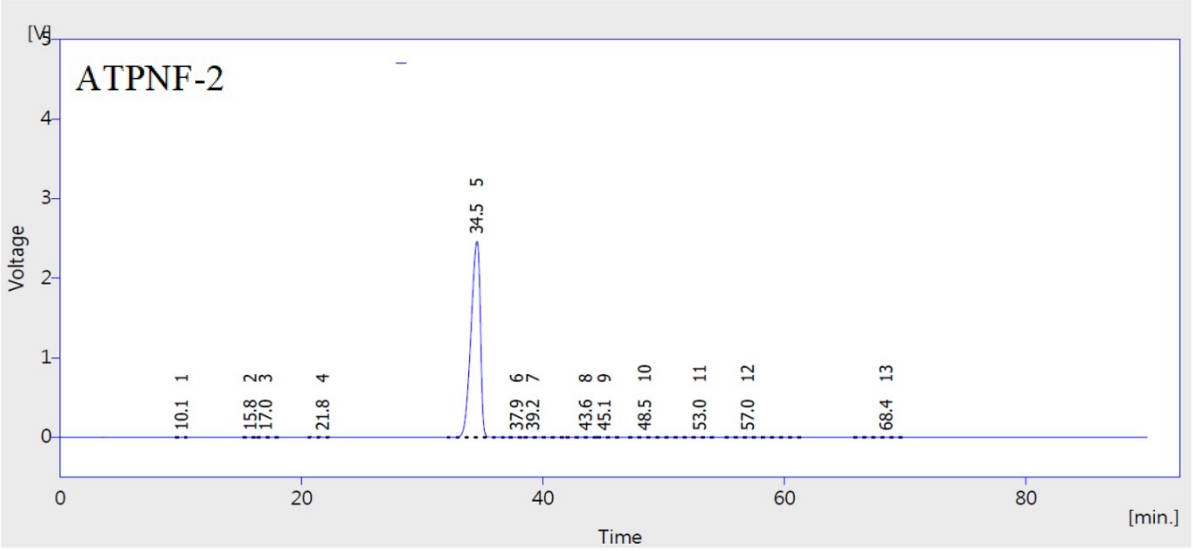

Column : Shiseido MG C18 4.6* 150m m, 5 um_Method : ACN_MeOH 7_3 0.5ml_90min